

Proteomic profiling of early degenerative retina of RCS rats

Zhi-Hong Zhu^{1,2}, Yan Fu^{1,2}, Chuan-Huang Weng^{1,2}, Cong-Jian Zhao^{1,2}, Zheng-Qin Yin^{1,2}

¹Southwest Hospital/Southwest Eye Hospital, Third Military Medical University, Chongqing 400038, China

²Key Lab of Visual Damage and Regeneration & Restoration of Chongqing, Chongqing 400038, China

Correspondence to: Cong-Jian Zhao and Zheng-Qin Yin. NO. 30, Gaotanyan Street, Shapingba district, Chongqing 400038, China. cj.zhao@yahoo.com; qinzyin@aliyun.com

Received: 2017-02-16 Accepted: 2017-04-06

Abstract

• **AIM:** To identify the underlying cellular and molecular changes in retinitis pigmentosa (RP).

• **METHODS:** Label-free quantification-based proteomics analysis, with its advantages of being more economic and consisting of simpler procedures, has been used with increasing frequency in modern biological research. Dystrophic RCS rats, the first laboratory animal model for the study of RP, possess a similar pathological course as human beings with the diseases. Thus, we employed a comparative proteomics analysis approach for in-depth proteome profiling of retinas from dystrophic RCS rats and non-dystrophic congenic controls through Linear Trap Quadrupole - orbitrap MS/MS, to identify the significant differentially expressed proteins (DEPs). Bioinformatics analyses, including Gene ontology (GO) and Kyoto Encyclopedia of Genes and Genomes (KEGG) pathway annotation and upstream regulatory analysis, were then performed on these retina proteins. Finally, a Western blotting experiment was carried out to verify the difference in the abundance of transcript factor E2F1.

• **RESULTS:** In this study, we identified a total of 2375 protein groups from the retinal protein samples of RCS rats and non-dystrophic congenic controls. Four hundred thirty-four significantly DEPs were selected by Student's *t*-test. Based on the results of the bioinformatics analysis, we identified mitochondrial dysfunction and transcription factor E2F1 as the key initiation factors in early retinal degenerative process.

• **CONCLUSION:** We showed that the mitochondrial dysfunction and the transcription factor E2F1 substantially contribute to the disease etiology of RP. The results provide a new potential therapeutic approach for this retinal degenerative disease.

• **KEYWORDS:** retinal degeneration; proteomics; mitochondrion; E2F1; MaxQuant; RCS rat

DOI:10.18240/ijo.2017.06.08

Zhu ZH, Fu Y, Weng CH, Zhao CJ, Yin ZQ. Proteomic profiling of early degenerative retina of RCS rats. *Int J Ophthalmol* 2017;10(6): 878-889

INTRODUCTION

Retinitis pigmentosa (RP) is a group of genetically mediated degenerative diseases, to which more than 80 genes related have been identified to date^[1-3]. Even though various genes contribute to retinal degeneration in different ways, they result in similar pathological features: progressive loss of rod and cone photoreceptors with progressive night blindness, and the gradual loss of the peripheral visual field, followed by the eventual loss of full field vision^[4]. Yet despite many mechanisms have been proposed to underlie this inherited neurodegenerative disease, there is still no satisfactory explanation for this phenomenon. Years ago, a mutation in HK1 gene encoding the hexokinase 1 was reported in several autosomal dominant RP families^[5]. Hexokinase 1 is an enzyme that believed to catalyze the phosphorylation of glucose to glucose-6-phosphate, the first step of glycolysis. Thus, we wondered if the abnormality of the glycolysis pathway may be involved in the development and occurrence of retinal degenerative. Alternatively, the role of mitochondria in inherited neurodegenerative diseases, such as Parkinson's disease, Alzheimer's disease and Huntington's disease, has been noted increasingly often recently. This prompted us to also assess the potential contribution of mitochondria in RP. Mitochondria are the driving force of life, as they provide the major energy source in cells through oxidative phosphorylation. Moreover, mitochondria also play an important role in mediating cell apoptosis, for example, by releasing pro-apoptotic factors such as cytochrome C, Smac/DIABLO, and endonuclease G into the cytosol^[6-8]. Consequently, mitochondrial dysfunction is a prime suspect for neuronal death. However, the precise role of mitochondria in photoreceptor cell death and the exact mechanism by which they exert their effects are still unknown.

Dystrophic RCS (RCS-rdy-p+) rats, which were established by the Royal College of Surgeons, are the first laboratory animal model for the study of RP. These rats possess a similar

Table 1 Retinal protein sample collection details

Sample IDs	Genotype	Age (postnatal days)	Retinas	Biological replicates	Technical replicates
RCS 18d	RCS	18	8	2	4
RCS 24d	RCS	24	8	2	4
RCS 30d	RCS	30	8	2	4
RCS 36d	RCS	36	8	2	4
CON 18d	rdy	18	8	2	4
CON 24d	rdy	24	8	2	4
CON 30d	rdy	30	8	2	4
CON 36d	rdy	36	8	2	4

pathological course as human beings with the diseases. The *merlk* gene mutation in the retinal pigment epithelium (RPE) causes a failure of phagocytosis in the deserted segment of photoreceptors, which leads to the death of photoreceptors^[9-10]. In dystrophic RCS rats, the first changes in the morphology of the retina can be observed at postnatal 14d, and the rod photoreceptor outer segments appear irregular in structure and contain some pyknotic nuclei. Next, an obvious reduction in the number of rod photoreceptors begins at postnatal 18d. This reduction is followed by a reduction in the number of cone photoreceptors, until they are all lost^[11]. In this study, we aimed to analyze retinal proteins obtained from this RP model rat, and compare it with that from normal congenic controls, to determine the potential significant factors molecular pathways involved in disease aetiology of RP.

To explore the potential molecular pathways involved in the early stages of RP, we took advantage of the label-free Orbitrap MS/MS-based proteomic approach^[12-15]. More specifically, we systematically analysed retinal proteins obtained from RCS rats and compared the data with that from normal congenic controls to screen changes in protein regulation. Considering that the retinal cells are still refining their synaptic wiring after the rat eye opens at postnatal 14d, late development process and RP-related degeneration may be occurring simultaneously. Therefore, we chose four different age groups (postnatal 18, 24, 30, and 36d) of RCS rats to explore the candidate biomarkers or molecular pathways involved in this disease.

MATERIALS AND METHODS

Materials Tris, Thiourea, Urea, DTT, DNase I and RNase A were all products of Sigma Company, USA. Cell lysis buffer, protein loading buffer, and the SDS-polyacrylamide gel preparing kit were obtained from Beyotime Biotechnology Company, China. Polyvinylidene fluoride membrane was purchased from Solarbio Science & Technology Corporation, USA. Trypsin was purchased from PROMEGA Corporation, China. All reagents and solvents were used without further purification.

Animals The study was approved by Institutional Animal Care and Use Committee of the Southwest Hospital, the Third Military Medical University, Chongqing, China. All procedures

were performed in accordance with the Association for Research in Vision and Ophthalmology Statement for the Use of Animals in Ophthalmic and Vision Research. According to the “3Rs” principles of animal research (replacement, reduction and refinement), a minimum number of rats needed to obtain reliable results and least invasive procedures to minimize pain and distress were used in this study. All participants are trained with the latest techniques to most effectively and humanely manage and care for rats. The dystrophic RCS (RCS-rdy-p+) rats and non-dystrophic congenic controls used in this study were bred in the animal facility of the Southwest Eye Hospital, the Third Military Medicine University, Chongqing, China. These rats were kept in the rooms with regular light-dark cycles (12:12h) that were controlled by a light timer.

A total of 32 rats were used in this study. Sixteen were dystrophic RCS rats, while the rest were non-dystrophic congenic controls. We divided them into four experimental cohorts according to postnatal days, 18, 24, 30 and 36d. All of the rats used in the study were asphyxiated in a CO₂ inhalation chamber and killed by cervical dislocation. The retinas were obtained from fresh eyeballs of the rats and immediately transferred into ice-cold phosphate buffered saline (PBS) (Table 1).

Protein Extraction and SDS-PAGE Retinal proteins were extracted from RCS rats and normal congenic controls at given time points. Considering that our interest is not on the individual but rather on the common changes in retinal degenerative process, pooled protein lysates from sets of 4 retinas per genotype at each age cohort were collected^[16]. Four protein lysate samples per age cohort were generated: two from RCS rat retina tissue (RCS, *n*=8), and two from normal congenic control (CON, *n*=8).

Freshly isolated rat retinas were suspended in hypotonic lysis buffer containing cell lysis buffer [20 mmol/L Tris, pH 7.5, 150 mmol/L NaCl, 1% Triton X-100, 2.5 mmol/L sodium pyrophosphate, 1 mmol/L EDTA, 1% Na₃VO₄, 0.5 µg/mL leupeptin, 1 mmol/L phenylmethanesulfonyl fluoride (PMSF)], 5 mol/L urea, 2 mol/L thiourea, 100 mmol/L DTT, 40 mmol/L Tris, 20 µg/mL DNase I, and 5 µg/mL RNase A. The samples were freeze-thawed three times in liquid nitrogen. The tissue

lysates were homogenized by ultracentrifugation for 30min at 10 000×g, 4 °C, followed by incubation at 4 °C for 2h. After incubation, the protein concentration of each individual tissue lysate was measured using the BCA protein assay (Beyotime Biotechnology Company, China) and bovine serum albumin as a protein standard. Then, tissue proteins (35 µg) were loaded on a 10% SDS-polyacrylamide gel for electrophoresis. The samples were stored at -20°C until proteomics analysis.

Mass Spectrometry Analysis To generate peptides suitable for mass spectrometry analysis, the samples were in-gel digested by adding trypsin, and digestion was carried out at 37 °C overnight. The EASY-nLC 1000 liquid chromatograph (LC) system (Thermo Fisher scientific, USA) was applied to acquire satisfying MS raw data using a two-column setup. The setup consisted of a 75-µm i.d. ×2-cm trap column and a 75-µm i.d. ×15-cm analytical nano-column. The sample injection volume was set to 5 µL. The LC system gradient was 5%-40% solvent B (A=99.9% water, 0.1% formic acid; B=99.9% acetonitrile, 0.1% formic acid) over 70min, 40%-80% solvent B over 5min, 80% solvent B for 5min and a reduction from 80% to 5% solvent B in 5min at a flow-rate of 250 nL/min.

Liquid chromatography was coupled with an LTQ-orbitrap Velos Pro mass spectrometer (Thermo Fisher scientific, USA), which is located at the Third Military Medicine University, Chongqing, China. Each peptide sample was measured four times. Nanospray ionization (NSI) was used with a spray voltage of 2.20 kV and a spray current of 0.65 µA. The Sheath Gas Flow Rate was set to -0.02, while the Aux Gas Flow Rate was -0.07, and the Sweep Gas Flow Rate was 0.20. The capillary temperature was set to 275.03 °C. The LTQ-orbitrap Velos Pro mass spectrometer was used in data-dependent MS acquisition mode. Acquisition was performed in the Orbitrap portion of the instrument for MS in the mass scan range of 350 to 2000 m/z at a resolution of 30 000 and in the linear ion trap portion of the instrument for MS/MS. The activate type was set to CID, with default charge state 2, isolation width 2 m/z, activation Q value of 0.25 and activation time of 15ms. The dynamic exclusion time was set to 60s.

Peptide Identification The raw files obtained from orbitrap MS/MS were imported into the Label-free Quantification (LFQ)-MaxQuant search engine (Ver. 1.5.3.8, <http://www.maxquant.org>)^[17-18] and MASCOT (Ver. 2.2) for identification and Label-free quantification of proteins.

For MASCOT configures, carbamidomethylation on cysteine was set as the fixed modification, while oxidation on methionine was set as the variable modification. Trypsin/P was set as the enzyme and, one trypsin missed cleavage was allowed. The false discovery rate (FDR) was set at lower than 1%.

For protein identification in MaxQuant, the database search engine Andromeda was used to search MS/MS spectra against the *Rattus norvegicus* database (updated at 2/08/2015, 29887

proteins) downloaded from the Uniprot database (<http://www.uniprot.org/proteomes/UP000002494>), with a tolerance level of 6 ppm for MS and 20 ppm for MS/MS. Trypsin/P was set as the enzyme, and two Max.missed cleavages were allowed. Protein N-terminal acetylation and oxidation of Methionines were set as variable modifications and carbamidomethylation of cysteines was set as a fixed modification. The Max.number of modifications per peptide was set as five, and contaminants were included. The “match between runs” feature was checked, with a match time window of 0.7min and an alignment time window of 20min. The FDR for protein level and peptide spectrum match (PSM) level were both set as 1%, and every peptide would be used only once in the protein identification process, in a razor peptide fashion. The minimum ratio count for protein quantification was set as two. Protein quantification was based on the MaxLFQ algorithm, using both unique and razor peptides for protein quantification, with the minimum ratio count for protein quantification setting as two. The default setting was used for all other configurations. Finally, the result was obtained from the proteinGroups.txt file in the column called “LFQ Intensity *etc.*”. This was calculated for each protein according to the MaxLFQ algorithm based on the (raw) intensities and normalized on multiple levels to ensure that the profiles of LFQ intensities across samples accurately reflected the relative amounts of the proteins^[18].

The mass spectrometry proteomics data have been deposited to the ProteomeXchange Consortium^[19] via the PRIDE^[20] partner repository with the dataset identifier PXD004094.

Statistical Analysis To assess the technical and biological variability of each retinal protein sample from each experimental group, we have calculated the Pearson correlation coefficients based on the LFQ intensities of each sample. ANOVA was performed using IBM SPSS statistics (version 19), and the LSD (least-significant-difference) method and the Boniferroni method were used as the correction method for multiple comparisons. To determine the statistically significantly differentially expressed proteins (DEPs) between RCS rats and normal controls at each experimental cohort, independent-samples Student’s two-tailed *t*-test was used to compare the intensities of each protein. A $P < 0.05$ was considered to be statistically significant. All of the statistics were calculated using IBM SPSS statistics (version 19). The data are shown as a heatmap, which was created by Hemi software^[21].

Bioinformatics Analysis The retinal proteins identified in RCS rats were categorized by protein class with PANTHER (Protein Analysis THrough Evolutionary Relationships) gene analysis tools (Ver. 9.0, <http://www.pantherdb.org/>)^[22-23]. The population distribution of the identified retinal proteins and statistically significant DEPs in cellular components (CC) was analyzed with PANTHER gene analysis tools.

To categorize the CC, biological processes (BP) and molecular functions (MF) of the identified statistically significantly DEPs in our data set, we imported the DEPs into STRING search engine (Ver. 10., <http://string-db.org>), a database of known and predicted protein interactions that provides biological information regarding protein interactions, Gene ontology (GO), and the Kyoto Encyclopedia of Genes and Genomes (KEGG) pathway^[24]. The enriched KEGG pathway mapping was performed on the KEGG (2.0, <http://www.genome.jp/kegg/>), a database resource with large-scale datasets obtained from high-throughput experimental technologies designed for understanding high-level functions and utilities of the biological system^[25].

Upstream regulatory analysis of significantly DEPs was performed to identify the key transcription factors involved in their regulation. A transcription factor and kinase search engine, Expression 2Kinases (X2K) (Ver. 1.6.1207. <http://www.maayanlab.net/X2K/>), which is based on a database of chromatin immune precipitation (ChIP)-seq/chip Enrichment Analysis (ChEA) and position weight Matrices (PWMs), was used^[26-27]. The graphic file obtained from Expression 2Kinases was edited by yEd Graph Editor (Ver. 3.14.4, <http://www.yworks.com/en/>).

Western Blot Analysis Proteins extraction and electrophoresis were performed as described in Section 2.3. In the following step, 10% SDS-polyacrylamide gel (Beyotime) was electrophoretically transferred to a polyvinylidene fluoride membrane (Solarbio, Beijing, China). After blocking in 5% nonfat dry milk in Tris-buffered saline (TBS) for 2h at room temperature, membranes were incubated overnight at 4 °C with primary rabbit polyclonal antibodies for E2F1 (1:500), and β -actin (1:1000) as internal control. All the primary rabbit polyclonal antibodies were diluted with primary antibody dilution buffer (Beyotime, China). After three washes with TBS for 10 min each, membranes were incubated with horseradish peroxidase (HRP)-conjugated goat anti-rabbit IgG (1:1 000) for 1h at room temperature. Antibody was diluted with secondary antibody dilution buffer (Beyotime, China). Protein bands were visualized using an enhanced chemiluminescence kit (BeyoECL Plus, Beyotime, China), and protein expression levels were analyzed using the Image J software^[28].

RESULTS

Protein Identification To explore the proteins related to early onset of retinal degeneration, comparative proteomic analysis was performed on retinal protein samples from dystrophic RCS rats (RCS) and non-dystrophic congenic controls (CON) at postnatal days 18, 24, 30 and 36d. The experimental workflow is illustrated in Figure 1A. Each genotype per age cohort contains two retinal protein samples (Sample #1, Sample #2) and each retinal protein sample contains tissues from two individual

animals (4 retinas). Proteomic analysis using LTQ-Orbitrap MS/MS is of high sensitivity, high resolution and high-mass accuracy but low repeatability. To increase the peptide coverage and experimental reliability, we carried out four independent experiments on each retinal protein sample. To evaluate the MaxLFQ algorithm integrated in the MaxQuant search engine, we also applied the MASCOT search engine, which is also frequently used to process MS spectral raw data. In contrast to MaxLFQ, MASCOT tends to calculate the significant threshold of ions score for every assigned peptide and only peptides that are higher than a significant threshold are considered as highly reliable. The relevant parameters and configurations are described in the Experimental Procedures.

The total numbers of RCS rat retinal proteins identified in sample #1 by MaxLFQ and MASCOT were 841 and 4518, respectively. Specifically, the numbers of proteins identified by MaxLFQ were 669, 552, 672 and 647, while that identified by MASCOT were 1489, 1153, 1283 and 1431, for each age cohort, respectively. However, although a greater number of proteins can be discovered by MASCOT, it appears to be less reliable compared with MaxLFQ, as low percentages (19.07%, 25.33%, 15.98% and 23.95%, respectively) of proteins were observed in four independent experiments, while high percentages (50.50%, 49.18%, 36.24% and 51.43%, respectively) of proteins were observed in only one experiment. In contrast, the percentages of proteins identified by MaxLFQ observed in four independent experiments were far higher (49.33%, 51.45%, 59.52% and 60.43%, respectively), while the percentages of that observed in only one experiment were far lower (10.76%, 19.20%, 15.77% and 15.46%, respectively) than MASCOT. Furthermore, the number of proteins observed in four independent experiments identified by MaxLFQ was slightly greater than that obtained by MASCOT (Figure 1B). Hence the proteome datasets outputted by MaxQuant search engine would be used for further analysis in this study.

The proteome datasets identified by MaxQuant consisted of 2523 protein groups, of which 37 protein groups were classified as “potential contaminant” and 24 protein groups as “reverse”, and 35 protein groups only identified in site. These so-called “potential contaminant” are common laboratory contaminant such as trypsin and human epidermal keratins, which may or may not be true contaminant but still should be ruled out in the following analysis. Finally, we have identified 2375 valid protein groups. To assess the reproducibility of the technical and biological replicates, Pearson correlation coefficient analysis was carried out based on the LFQ intensities with each experimental group. Pearson correlation coefficients were represented in Table 2. The result revealed Pearson correlation coefficients between 0.64 and 0.99, and indicated that biological replicates and analytical replicates had a relatively high degree of reproducibility.

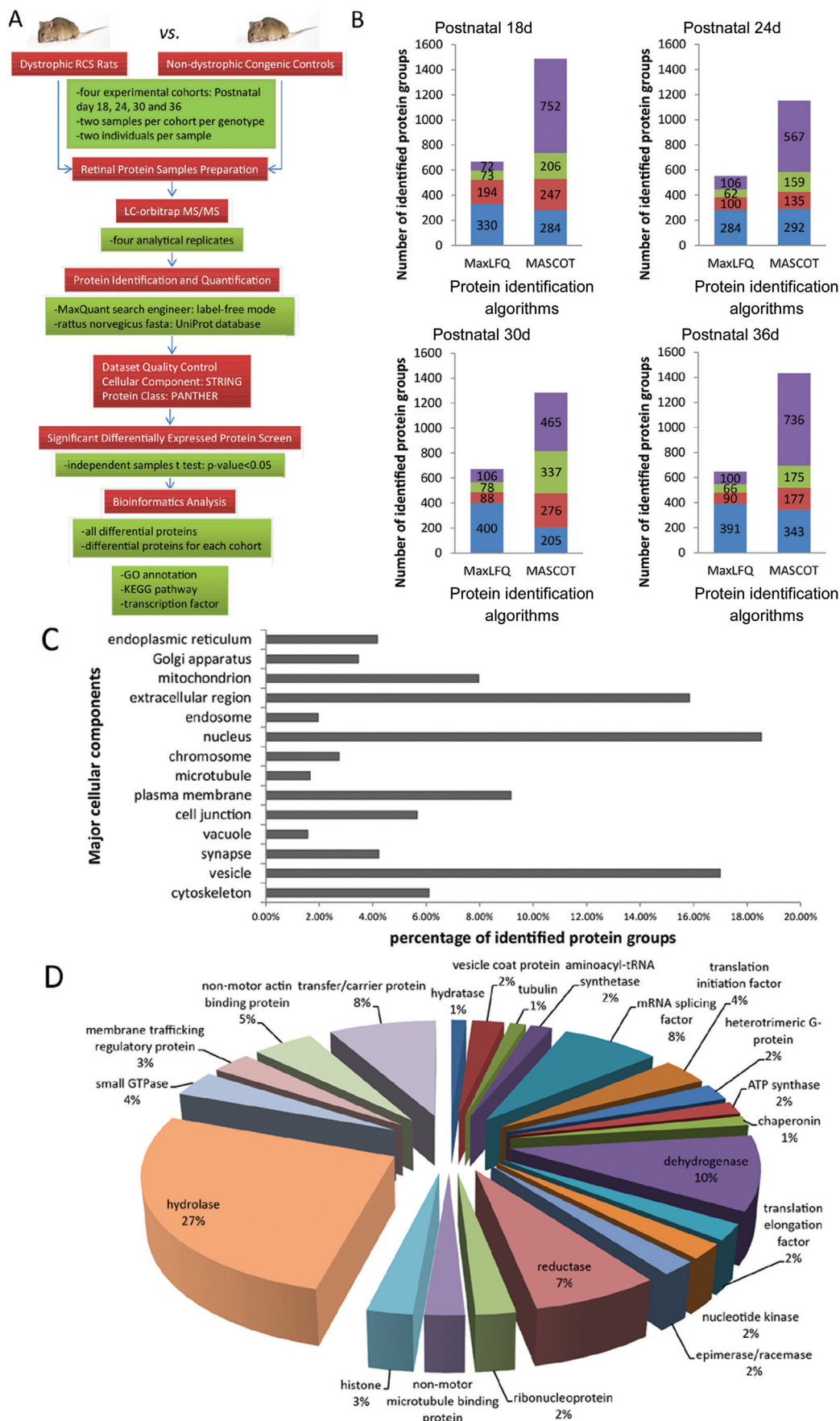


Figure 1 Protein identification of retina samples from model rats using LC-orbitrap MS/MS The process of sample preparation, data acquisition, and data analysis is shown in the flowchart (A). Proteins from RCS rat retina in sample #1 identified by MaxLFQ and MASCOT yield 841 (669, 552, 672 and 647 in each age cohort) and 4518 (1489, 1153, 1283 and 1431 in each age cohort) protein groups, respectively (FDR<1%). Blue column represents the number of protein groups observed in every experiment, while red column in three and olive column in two, and violet column in only one (B). The percentage of major cellular components is presented as a bar chart and shows the population distributions of all identified protein groups in various subcellular compartments (C). All of the retinal proteins of RCS rats identified by MaxLFQ were categorized by Protein Class with PANTHER database, ranking hydrolase proteins to the top with the largest proportion (D).

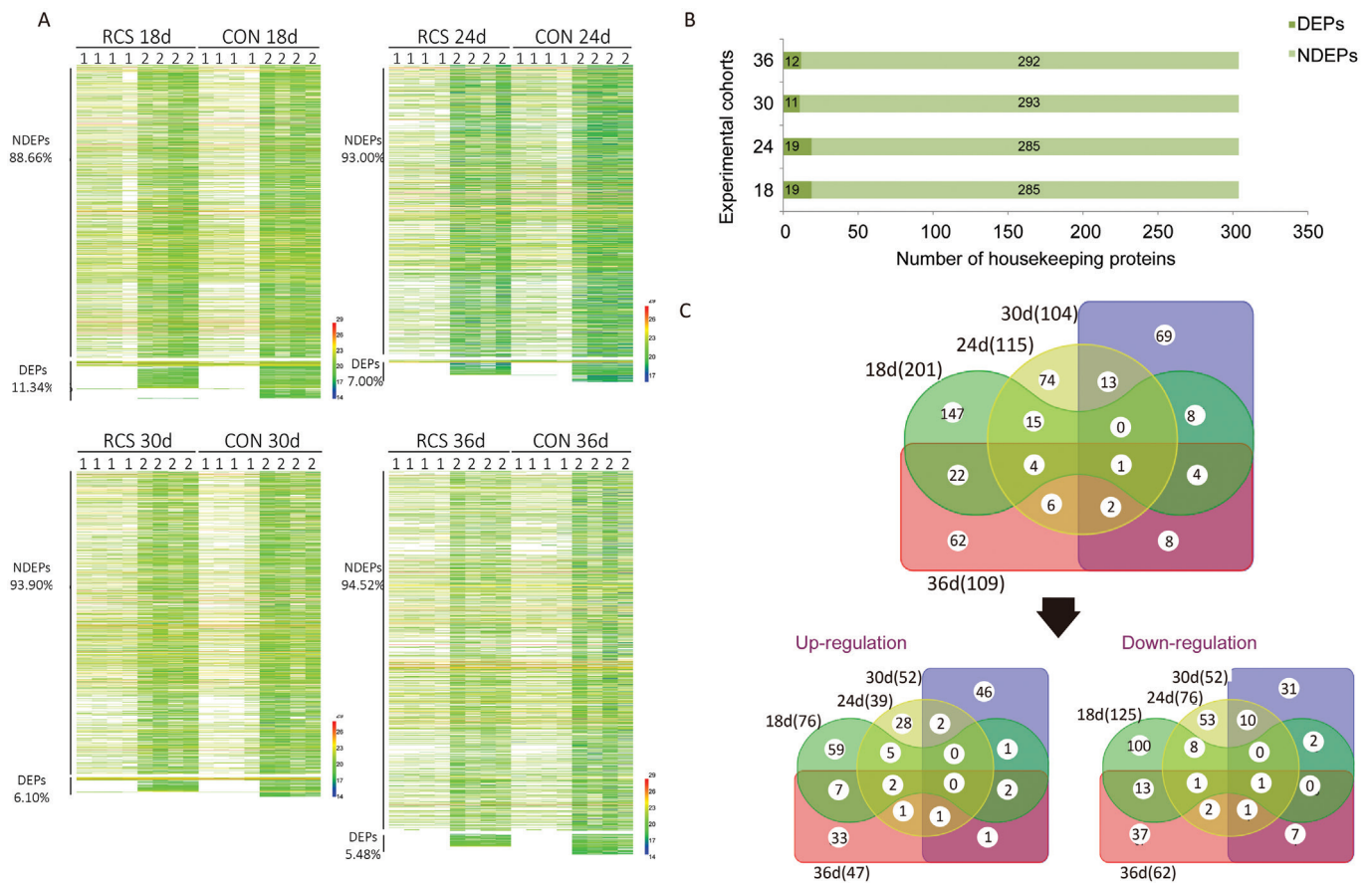


Figure 2 Significantly differentially expressed proteins identified by MaxLFQ A total of 2375 protein groups were discovered by MaxLFQ. Specifically, 1746, 1658, 1704 and 2006 protein groups were discovered in the 18, 24, 30 and 36d age cohorts, respectively. Student's *t*-test was performed using IBM SPSS statistics, and proteins with a *P*-value <0.05 in both samples were considered as statistically significant. There were 201, 115, 104 and 109 significantly differentially expressed proteins (DEPs) in the 18, 24, 30 and 36d age cohorts, respectively(A). 304 housekeeping proteins were observed in this study. Fewer of them showed differential abundance (B). The Venn diagram shows the number of DEPs in each age cohort, and the overlap among the four age cohorts is also shown (C).

Table 2 Pearson correlation coefficients between the LFQ (label-free quantification) intensities from the biological and technical replicates in all experimental groups

Experimental groups	Correlation coefficients in biological replicates	Correlation coefficients in technical replicates
RCS 18d	0.7668-0.8721	0.9040-0.9976
RCS 24d	0.7081-0.8536	0.9018-0.9893
RCS 30d	0.7802-0.8930	0.9195-0.9933
RCS 36d	0.6465-0.8468	0.9036-0.9931
CON 18d	0.6891-0.8902	0.8549-0.9951
CON 24d	0.7953-0.9169	0.9113-0.9957
CON 30d	0.8004-0.9116	0.9497-0.9966
CON 36d	0.7154-0.8777	0.9425-0.9937

To evaluate the population distribution of the identified retinal proteins, we imported the total 2375 protein groups into PANTHER gene analysis tools. As shown in Figure 1C, nucleus, vesicle and extracellular region accounted for the largest proportion of annotation proteins. All the protein groups were categorized by protein class through PANTHER gene analysis tools, ranking hydrolase protein (27%) to the top. In addition, dehydrogenase (10%), transfer/carrier protein (8%), mRNA splicing factor (8%) and reductase (7%) were also identified

as major protein classes. Other than these protein classes, a small percentage (1%) of proteins were also determined to be chaperonin, tubulin and hydratase (Figure 1D).

Significantly Differentially Expressed Protein Analysis Between RCS and Controls The proteome datasets consisted of 1746, 1658, 1704 and 2006 protein groups for the 18, 24, 30 and 36d cohorts, respectively. Data were represented as heatmap in Figure 2A.

ANOVA was performed on each four independent experimental proteome datasets to confirm the homogeneity of the four independent experimental datasets. All of the *P*-values obtained were greater than 0.05, indicating that there was a good agreement between all of the datasets derived from one same sample. Thus, we were able to use independent-samples Student's *t*-test to analyze the differences between RCS and controls from each age cohort based on these datasets. Two separate comparisons between RCS and CON were performed based on pooled proteome datasets sample #1 and sample #2. Only proteins with a *P*<0.05 in both samples were considered to be statistically significant. Four hundred thirty-four significant DEPs were identified in this study. Specifically, the numbers of DEPs were 201, 115, 104 and 109 for 18, 24, 30 and 36d cohorts, respectively.

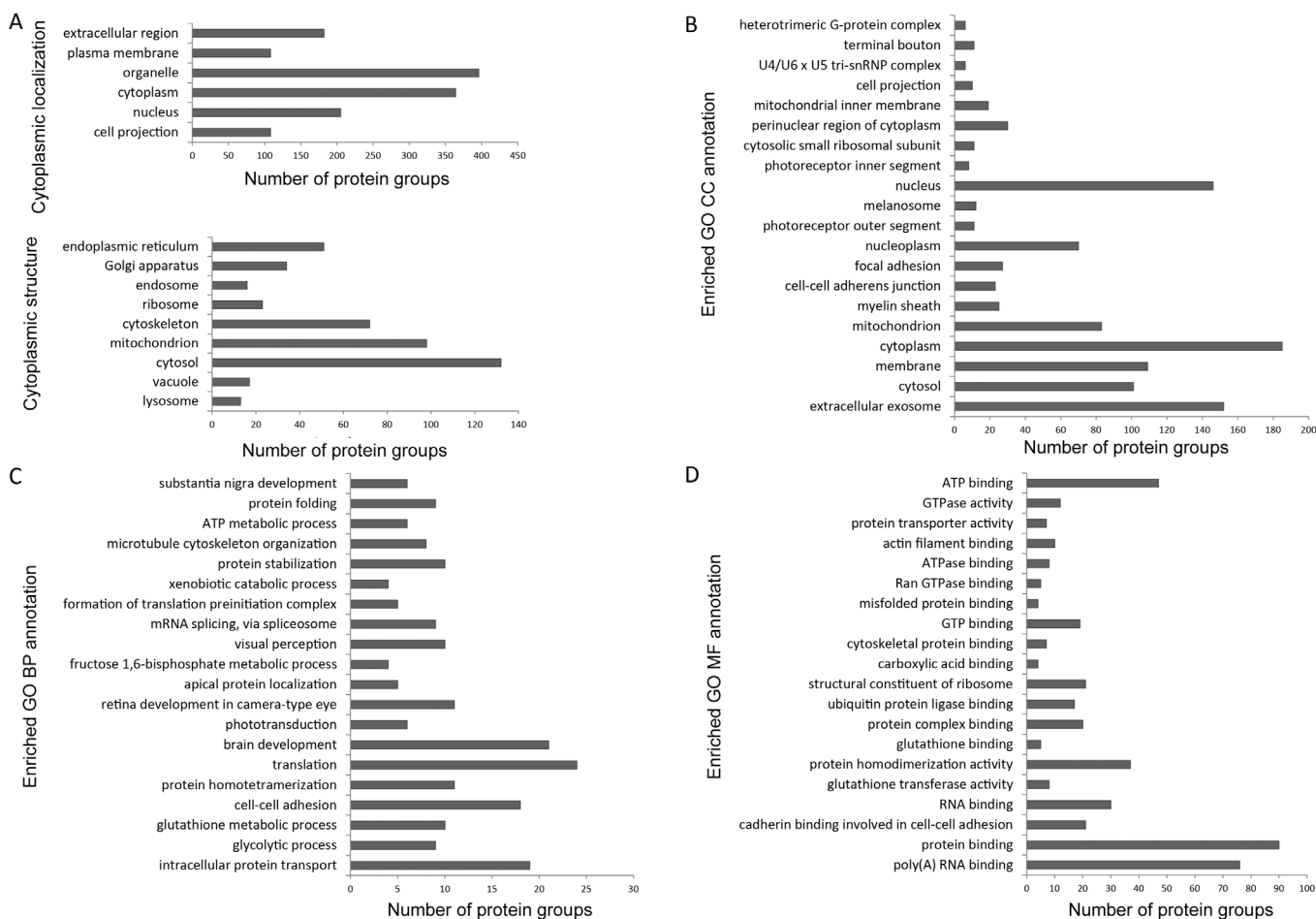


Figure 3 Functional enrichment analysis of GO annotation The data are presented as bar charts showing the distribution patterns of proteins in six major subcellular components (search in PANTHER database), including the cell projection, cytoplasm, nucleus, organelle, plasma membrane and extracellular region, and more specifically, the distribution patterns of proteins in detailed cytoplasmic structures (A). The top 20 significantly enriched GO cellular component (CC) categories (B), biological process (BP) categories (C) and molecular function (MF) categories (D) are shown (search in STRING database). Data was ranked by *P*-value corrected with the Boniferroni method.

To check the housekeeping proteins, 304 housekeeping proteins have been identified, including the ribosomal proteins, histones, translation factors, tRNA synthetases, heat shock proteins, cell cycle proteins, and citric acid cycle enzymes. Despite a few proteins (less than 7%) having a slight significant differential regulation at each age cohort, most of the housekeeping proteins have relatively steady abundance levels, *e.g.* Tpi1, Sdha, H2afz/H2afv, Rpsa, Atp1b2/Atp2b1/Atp5o/Atp6v1a, *etc.* (Figure 2B). These results further demonstrated the quality of MS data and convinced us that the proteome datasets from RCS rat are indeed controlled with the properly timed normal congenic controls at every given time point.

Of the total 434 protein groups, up regulation was observed in the abundance of 76, 39, 52 and 47 proteins (18, 24, 30 and 36d cohort, respectively), while down regulation was observed in 125, 76, 52 and 62 proteins (Figure 2C). One protein groups (Clic 6, a member of chloride intracellular channel family which is best known for interaction with D-like receptors) displayed statistically significant down-regulation in abundance levels ($P < 0.05$) through all four age cohorts. One protein groups (Sugt1, protein SGT1 homolog which may play

a role in ubiquitination and subsequent proteasomal degradation of target proteins) displayed statistically significantly down-regulation and one protein (Hp1bp3, Heterochromatin protein 1-binding protein 3 which is component of heterochromatin and may play a role in hypoxia-induced oncogenesis) displayed statistically significantly up-regulation in abundance levels ($P < 0.05$) in the last three age cohorts (24, 30 and 36d).

Enrichment Analysis of GO Annotation and KEGG Pathway

Using the PANTHER gene analysis tools, these DEPs were parsed into six major subcellular components, composed of the cell projection, cytoplasm, nucleus, organelle, plasma membrane and extracellular region. Subsequently, their location in detailed cytoplasmic structures was also determined (Figure 3A). The cytosol (132 proteins), mitochondrion (98 proteins) and cytoskeleton (72 proteins) occupy the highest proportion of total DEPs. Specifically, 37 proteins were localized on the mitochondrial membrane (25 proteins on the inner membrane and 10 proteins on the outer membrane), five proteins were localized in the mitochondrial intermembrane space and 16 proteins localized in the mitochondrial matrix.

To obtain biological information on their cellular component (CC), molecular function (MF) and biological process (BP) of the DEPs between RCS and control, we subjected the total 434 DEPs to GO enrichment analysis with STRING search engine. The enriched GO CC annotation also suggested that extracellular exosome, cytosol, membrane, cytoplasm and mitochondrion were identified as the top five enriched categories ($P < 0.001$) (Figure 3B). However, we were not surprised to find that photoreceptor outer segment and photoreceptor inner segment, locations where retinal degenerative changes primarily occur at early stage, were also demonstrated as significantly over-represented subcellular locations.

Furthermore, we have carried out GO BP and MF enrichment analyses. Intracellular protein transport, glycolytic process and glutathione metabolic process were ranked as the top 3 GO BP categories ($P < 0.001$), suggesting the prominent biological meaning of cytosol and mitochondrion in the disease (Figure 3C). Glycolytic process is a chemical reaction of converting a carbohydrate into pyruvate and generating concomitant production of small amounts of ATP and NADH, and the central pathway that produces important precursor metabolites such as six-carbon compounds, three-carbon compounds and Acetyl-CoA. Dysfunction of glycolytic process may be the reason inducing cellular metabolic disorders and eventually cell apoptosis. Glutathione, the tripeptide glutamylcysteinylglycine, has a specific role in the reduction of hydrogen peroxide (H_2O_2) and oxidized ascorbate. Dysfunction of glutathione metabolic process implied the content change of reactive oxygen species (ROS).

Enrichment analysis of GO MF indicated that poly (A) RNA binding, protein binding and cadherin binding involved in cell-cell adhesion ($P < 0.001$) were ranked as the top three molecular function categories (Figure 3D). What should be noteworthy is that glutathione transferase activity and glutathione binding were also detected as over-represented categories, which may be activated as an antioxidant.

Moreover, to explore the metabolic pathways of DEPs, enriched KEGG pathway analysis on the total 434 DEPs has been performed. Top 20 enriched KEGG pathways are shown in Figure 4A. As expected, phototransduction was ranked to the top with highest enrichment significance ($P = 2.40e-7$). The progressively loss of rod and cone photoreceptors surely led to dysfunction of photo transduction pathway which is accomplished by photoreceptor. Several proteins that participated in phototransduction process, such as Gngt1, Rcvrn, Guca1a, Gnat1, Rgs9 and Guca1b, have a significant down-regulation in 30d and 36d cohort, while other proteins, such as Pde6a, Gucy2f, Gucy2e/Gucy2d, Rho, Sag, Grk1, Cnga1, Cngb1 and Slc24a1, were identified as significant down-regulation only in sample #2 with a non-significant down-regulation in sample #1.

In addition, carbon metabolism, especially glycolysis/gluconeogenesis, was also detected as over-represented category with high enrichment significance ($P < 0.001$). The enrichment analysis of KEGG pathways for each age cohort indicated that at early stages (18d and 24d cohort), glycolysis/gluconeogenesis was identified as the most prominent pathway, suggesting the important role of glycolysis/gluconeogenesis in the initiation and occurrence of retinal dystrophy. In addition, subsequently in the 30d and 36d cohort, phototransduction becomes the major significantly abnormal pathway, indicating the progressively loss of rod and cone photoreceptors with the development of retina degenerative (Figure 4B). Specifically, enzymes involved in glycolysis/gluconeogenesis pathway, including Hk1/Hk2, Pfkfb1/Pfkfb3, Aldoc, Gapdh, Eno2 and Dld, have a significant up-regulation in protein abundance level in 18d cohort (Figure 4C). What is more, the conversion of three-carbon compounds from glyceraldehyde-3P to pyruvate is the core part of biosynthesis of amino acid, which is also detected as an over-represented pathway with high enrichment significance ($P < 0.001$). However, the abundance of these significant up-regulated proteins was nearly normal in subsequent age cohorts. Enriched GO CC and BP analysis on DEPs in 18d cohort are shown in Figure 4D. Extracellular exosome, cytosol, membrane, mitochondrion and cytoplasm were identified as top five enriched CC, while glycolytic process, glutathione metabolic process, cell-cell adhesion, translation and ATP metabolic process were identified as top five enriched BP.

Upstream Regulatory Analysis To predict the upstream transcription factors of the identified DEPs, DEP data were input into the X2K software. We obtained a set of enriched upstream regulators, including transcription factor MYC, E2F1 and CCND1 (Figure 5A). MYC, E2F1 and CCND1 regulate the abundance level of a large amount of DEPs. E2F1, a transcription factor which mediates cell proliferation and TP53/p53-dependent apoptosis, is mainly responsible for regulation of enzymes participated in carbon metabolism and biosynthesis of amino acid in this study (Figure 5B). Given that carbon metabolism and biosynthesis of amino acid were the major over-represented pathways in 18d and 24d cohorts, we supposed that E2F1 is the key regulator in rod and cone photoreceptors apoptosis at early stage of RP. The difference in the expression of E2F1 was further verified by Western blotting analysis (Figure 5C). As predicted, E2F1 were significantly up-regulated in RCS.

DISCUSSION

RCS rat is an animal model of RP that share similar pathological processes observed in RP patients, thereby providing a unique model to study the early biochemical changes in this disease. In this study, we are the first performing a systematic comparative proteomics analysis based on orbitrap MS/MS

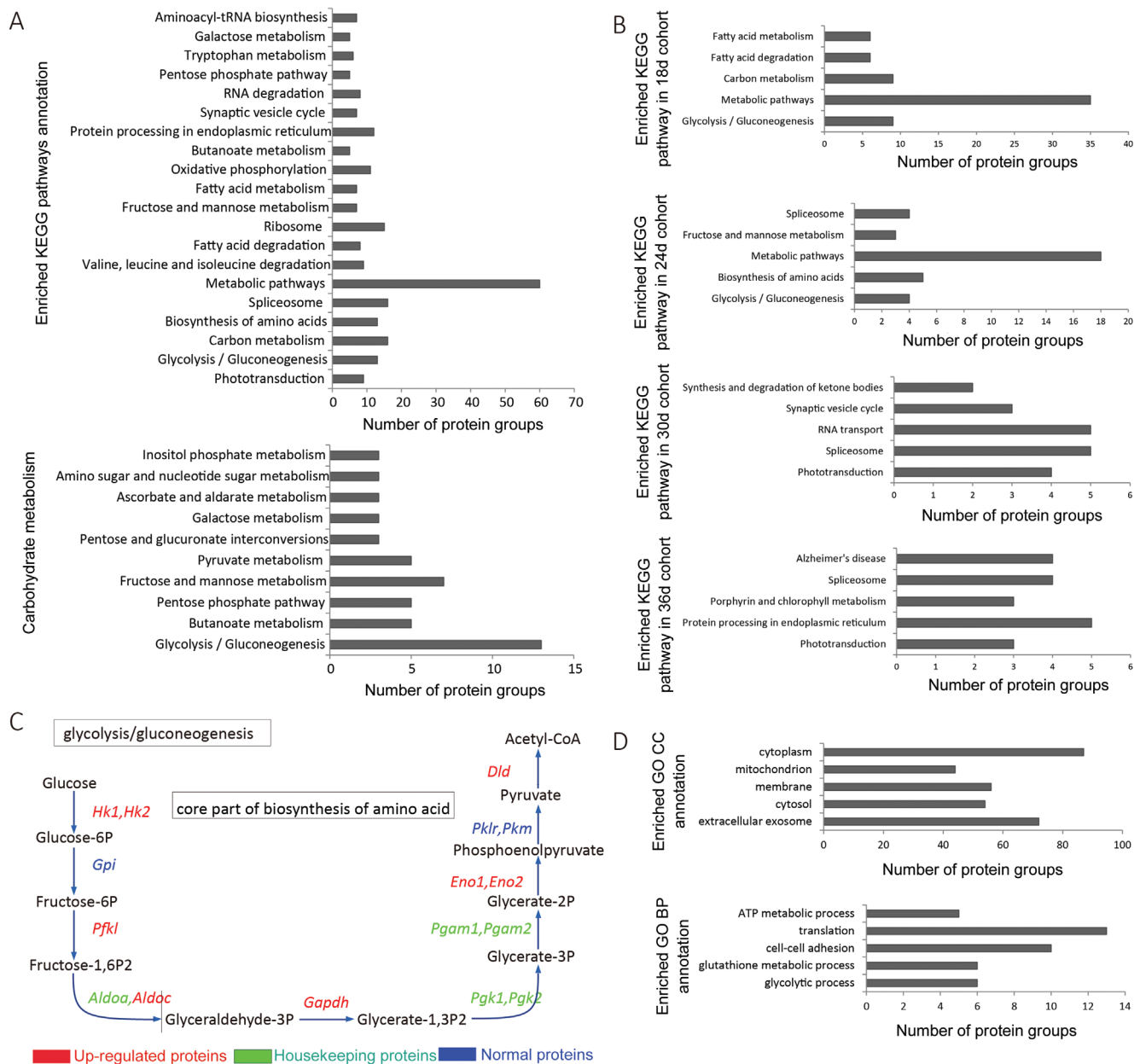


Figure 4 Enriched KEGG pathway analysis of significantly differentially expressed proteins and mapping of the glycolysis/gluconeogenesis pathway Enriched KEGG pathways categories were presented as a bar chart of 20 over-represented pathways. Carbohydrate metabolism pathways (16 DEPs), especially glycolysis/gluconeogenesis (13 DEPs), has drawn great attention with a high enrichment significance (A). The top five enriched KEGG pathways annotation for each age cohort show that the protein groups involved in glycolysis/gluconeogenesis pathway may play an important role at early stage of retinitis pigmentosa (B). In 18d cohort, the DEPs involved in glycolysis/gluconeogenesis were significantly up-regulated (C). Enrichment analysis of GO CC and BP annotation in 18d cohort were presented as a bar chart (D). Data were ranked by *P*-value corrected with the Boniferroni method.

label-free quantification approach on dystrophic RCS rats and non-dystrophic congenic controls, with the aim of finding out the candidate initiation factors and regulators that are involved in early disease aetiology. To overcome error from biological variance and technical variance, two separate protein lysate samples consisting of four retinas each (obtained from two individual rats) per genotype were analyzed at four different age cohorts. This strategy of sample subpooling preparation could not only reduce biological variance by averaging discrepancies from each individual, but also conduct the appropriate comparative analysis on retina proteome from RCS rats and normal congenic controls^[29-32].

In this study, we identified a total of 2375 retinal protein groups from RCS rats by MaxLFQ algorithm integrated in MaxQuant search engine. 434 protein groups were identified as significantly difference in abundance from the normal controls, and about half of them were discovered in the 18 d cohort, suggesting that many complicated biochemical reactions primarily occurred at the early stage of disease, with the result of relevant pathological processes such as rod and cone photoreceptors cell death. Approximately 1/4 of DEPs were localized in the mitochondrion, and in detail, approximately 1/4 of them were located on the inner membrane, which is

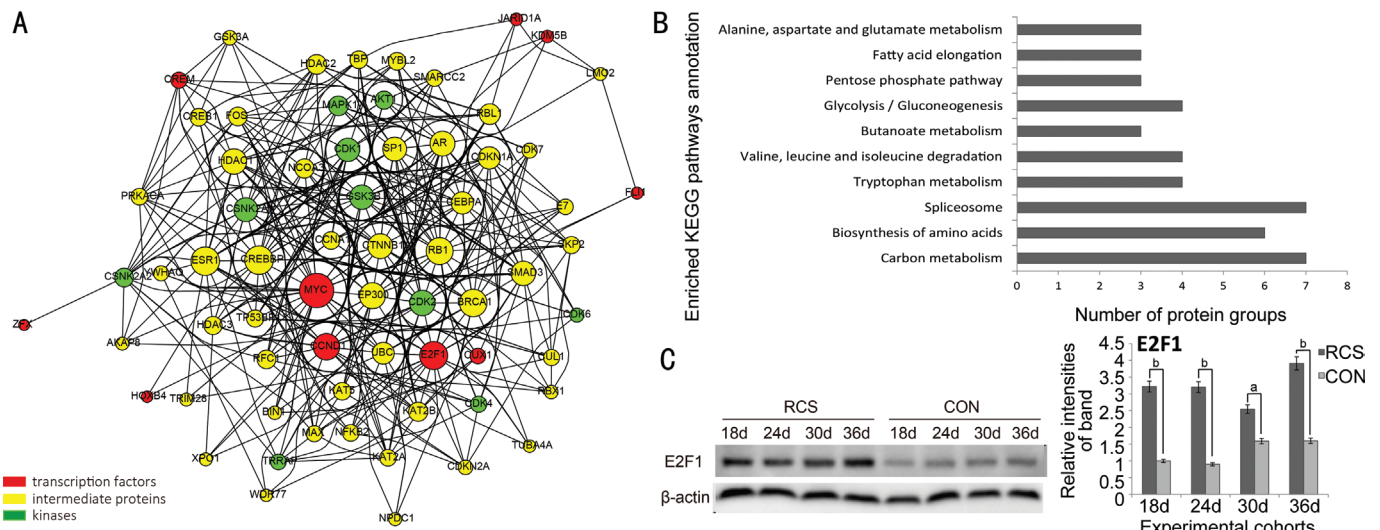


Figure 5 Upstream regulatory analysis of significantly differentially expressed proteins and verification by Western blot Of all of the candidate transcription factors, MYC, E2F1 and CCND1 occupied the highest proportion of the upstream regions of the differentially expressed proteins (A). Enriched KEGG pathway analysis on DEPs regulated by E2F1 is presented as a bar chart (B). Western blot analysis with E2F1 antibody was performed. Data are shown as mean±SD from three densitometry evaluation; ^a*P*<0.05; ^b*P*<0.005. β-actin was used for internal control (C).

the site for oxidative phosphorylation. On the other hand, cytosol and membrane proteins were also occupy over 1/4 of DEPs. In the enrichment analysis of KEGG pathway, phototransduction was identified as the most enriched pathway with significantly down-regulation, as no surprise. In addition, glycolysis/gluconeogenesis was also identified as over-represented pathway. This metabolic pathway was also detected as the most prominent pathway in 18d and 24d cohort. Certain cytosolic proteins that participated in the glycolysis/gluconeogenesis pathway were significantly up-regulated in the 18d cohort. Glycolytic process and glutathione metabolic process were also detected as enriched BP in 18d cohort. Combination of the above enriched GO annotation and KEGG pathway analysis result suggested that mitochondrial dysfunction and abnormalities in glycolytic metabolism and biological oxidation are likely to play an important role in retinal remodeling and degeneration, especially in the early stages of the disease.

In addition to their critical role in life support, mitochondria are also involved in apoptosis and have been implicated in neurodegenerative diseases, including Parkinson's disease, Huntington's disease, Alzheimer's disease and neuropathy ataxia RP^[33]. Several studies on the role of mitochondria in neurodegenerative diseases have already been reported. For example, Sanges *et al*^[34] identified two apoptotic pathways involving the mitochondria and endoplasmic reticulum in degenerating neurons in Rd1, another model animal of RP. In our study, abnormal expressed proteins in mitochondria were pretty significant. Thus, we hypothesize that mitochondrial dysfunction is the key initiation factor in RP. In RCS rat retina, *mertk* gene mutation in the RPE causes a failure to

phagocytosis the outer rod segment discs that have been shed, which leads to an accumulation of outer rod segment debris. As a result, rod photoreceptor stopped developing and started degenerating before cellular maturation completes. During rod photoreceptor degeneration, damage may presented in mitochondria, leading to increased generation of ROS, which can aggravate cellular inflammation and injury^[35]. With the increasing generation of ROS, rod and cone photoreceptors underwent apoptosis or programmed cell death^[36-37]. Moreover, mitochondrial dysfunction could also cause an imbalance of calcium homeostasis, or the release of cytochrome C into the cytosol, which can bind to Apaf1 and pro-caspase 9 to form the apoptosome and give rise to a downstream caspase cascade, ultimately resulting in cell apoptosis^[38].

Mitochondrial dysfunction can also impact the energy metabolism. As is well known, the mitochondrion is the most prominent site of energy production for cell. Impairment of mitochondria would lead to decreased generation of energy currency of the cell, *i.e.* ATP, resulting in compensatory hyperactive of glycolytic process. Glycolysis pathway is another crucial energy metabolic pathway taking place in cytoplasm, and generating small amounts of ATP and NADH. It is the process of converting glucose into pyruvate, an important precursor metabolite for Acetyl-CoA, which is produced by the oxidative decarboxylation of pyruvate in the TCA cycle^[39-40]. In this study, we observed a significant up-regulation in enzymes involved in glycolysis pathways at 18d cohort. We supposed that it might be the result of mitochondrial dysfunction. However, with the progressive loss of rod and cone photoreceptor, the compensatory effect of glycolysis decreased, and finally became decompensatory. In

addition, photo transduction later began to reach dysfunction. Furthermore, rod and cone photoreceptor cell death would lead to decreased rod oxygen consumption and hyperoxia within the retina, resulting in more increased generation of ROS.

Upstream regulatory analysis on total DEPs indicated that E2F1 plays a potential role in the retinal degenerative process in RCS rats. The up-regulation of E2F1 in RCS rat at 18d cohort has been verified by Western blot analysis. Thus, we wonder if abnormal hyperactivity of E2F1 was the key regulator in occurrence of retina degenerative. A recent study by Zencak *et al*^[41] seems to confirm our conjecture. His research demonstrated that deletion of E2F1 transiently prevented photoreceptor loss in the Rd1 mouse model. Furthermore, E2F1 has been shown to contribute to neuronal death in Parkinson's disease^[42]. Given that E2F1 plays a central role in regulating the cell cycle, it may participate in neuronal death in various neurodegenerative diseases, including RP. E2F1 may be a potential therapeutic molecular target in RP.

Since great progress has been made in new instrumentation developments, fragmentation methods and retrieval strategies, mass spectrometry-based label-free quantification proteomics has become an indispensable technology for insights into complex BP such as physiological/pathological metabolism in disease. With the high sensitivity, high mass accuracy, good dynamic range, and the ability to perform large-scale analyses, we could profile the comparative proteomics in retina between dystrophic RCS rats and non-dystrophic congenic controls for in-depth analysis of underlying disease mechanism. However, qualitatively and quantitatively of label free proteomics remains an enormous challenge. Other than labelling methods such as iTRAQ, Label-free quantitation strategies required that sample must be analysed repeatedly for a high level of reproducibility and reliability. In this study, low detection rate and repetition rate of many low abundance proteins was often confused. It is very important to increase the number of biological and technical replicates to generate robust results.

In conclusion, comparative proteomic analysis can enable the identification of protein differences between two samples, especially with the help of rapidly growing bioinformatics technologies. Further development of these technologies will undoubtedly increase the analytic depth and width of scientific research. Our study demonstrates the critical abnormality of mitochondria and transcription factor E2F1 in the initiation of RP. Additional studies are required to validate these results and elucidate the molecular mechanism underlying RP.

ACKNOWLEDGEMENTS

We would like to thank Dr. Huang Y and Kuang YS for their help with MS analysis.

Foundations: Supported by the National Nature Science Foundation of China (No.81130017); National Basic Research Program of China (973 Program, No.2013CB967002).

Conflicts of Interest: Zhu ZH, None; Fu Y, None; Weng CH, None; Zhao CJ, None; Yin ZQ, None.

REFERENCES

- 1 Liu MM, Zack DJ. Alternative splicing and retinal degeneration. *Clin Genet* 2013;84(2):142-149.
- 2 Daiger SP, Sullivan LS, Bowne SJ. Genes and mutations causing retinitis pigmentosa. *Clin Genet* 2013;84(2):132-141.
- 3 Ripps H. Cell death in retinitis pigmentosa: gap junctions and the 'bystander' effect. *Exp Eye Res* 2002;74(3):327-336.
- 4 Hartong DT, Berson EL, Dryja TP. Retinitis pigmentosa. *Lancet* 2006;368(9549):1795-1809.
- 5 Sullivan LS, Koboldt DC, Bowne SJ, Lang S, Blanton SH, Cadena E, Avery CE, Lewis RA, Webb-Jones K, Wheaton DH, Birch DG, Coussa R, Ren H, Lopez I, Chakarova C, Koenekoop RK, Garcia CA, Fulton RS, Wilson RK, Weinstock GM, Daiger SP. A dominant mutation in hexokinase 1 (HK1) causes retinitis pigmentosa. *Invest Ophthalmol Vis Sci* 2014;55(11):7147-7158.
- 6 Comitato A, Sanges D, Rossi A, Humphries MM, Marigo V. Activation of Bax in three models of retinitis pigmentosa. *Invest Ophthalmol Vis Sci* 2014;55(6):3555-3562.
- 7 Ikeda HO, Sasaoka N, Koike M, Nakano N, Muraoka Y, Toda Y, Fuchigami T, Shudo T, Iwata A, Hori S, Yoshimura N, Kakizuka A. Novel VCP modulators mitigate major pathologies of rd10, a mouse model of retinitis pigmentosa. *Sci Rep* 2014;4:5970.
- 8 Hartong DT, Dange M, McGee TL, Berson EL, Dryja TP, Colman RF. Insights from retinitis pigmentosa into the roles of isocitrate dehydrogenases in the Krebs cycle. *Nat Genet* 2008;40(10):1230-1234.
- 9 Tso MO, Zhang C, Abler AS, Chang CJ, Wong F, Chang GQ, Lam TT. Apoptosis leads to photoreceptor degeneration in inherited retinal dystrophy of RCS rats. *Invest Ophthalmol Vis Sci* 1994;35(6):2693-2699.
- 10 D'Cruz PM, Yasumura D, Weir J, Matthes MT, Abderrahim H, LaVail MM, Vollrath D. Mutation of the receptor tyrosine kinase gene *Mertk* in the retinal dystrophic RCS rat. *Hum Mol Genet* 2000;9(4):645-651.
- 11 Strauss O, Stumpff F, Mergler S, Wienrich M, Wiederholt M. The Royal College of Surgeons rat: an animal model for inherited retinal degeneration with a still unknown genetic defect. *Acta Anat (Basel)* 1998;162(2-3):101-111.
- 12 Ning K, Fermin D, Nesvizhskii AI. Comparative analysis of different label-free mass spectrometry based protein abundance estimates and their correlation with RNA-Seq gene expression data. *J Proteome Res* 2012;11(4):2261-2271.
- 13 Hu Q, Noll RJ, Li H, Makarov A, Hardman M, Graham Cooks R. The Orbitrap: a new mass spectrometer. *J Mass Spectrom* 2005;40(4):430-443.
- 14 Cheng FY, Blackburn K, Lin YM, Goshe MB, Williamson JD. Absolute protein quantification by LC/MS(E) for global analysis of salicylic acid-induced plant protein secretion responses. *J Proteome Res* 2009;8(1):82-93.
- 15 Polpitiya AD, Qian WJ, Jaitly N, Petyuk VA, Adkins JN, Camp DG 2nd, Anderson GA, Smith RD. DAnTE: a statistical tool for quantitative analysis of -omics data. *Bioinformatics* 2008;24(13):1556-1558.

- 16 Kikuchi T, Hassanein M, Amann JM, Liu Q, Slebos RJ, Rahman SM, Kaufman JM, Zhang X, Hoeksema MD, Harris BK, Li M, Shyr Y, Gonzalez AL, Zimmerman LJ, Liebler DC, Massion PP, Carbone DP. In-depth proteomic analysis of non-small cell lung cancer to discover molecular targets and candidate biomarkers. *Mol Cell Proteomics* 2012;11(10):916-932.
- 17 Cox J, Mann M. MaxQuant enables high peptide identification rates, individualized p.p.b.-range mass accuracies and proteome-wide protein quantification. *Nat Biotechnol* 2008;26(12):1367-1372.
- 18 Cox J, Hein MY, Luber CA, Paron I, Nagaraj N, Mann M. Accurate proteome-wide label-free quantification by delayed normalization and maximal peptide ratio extraction, termed MaxLFQ. *Mol Cell Proteomics* 2014;13(9):2513-2526.
- 19 Vizcaino JA, Deutsch EW, Wang R, Csordas A, Reisinger F, Rios D, Dienes JA, Sun Z, Farrah T, Bandeira N, Binz PA, Xenarios I, Eisenacher M, Mayer G, Gatto L, Campos A, Chalkley RJ, Kraus HJ, Albar JP, Martinez-Bartolomé S, Apweiler R, Omenn GS, Martens L, Jones AR, Hermjakob H. ProteomeXchange provides globally coordinated proteomics data submission and dissemination. *Nat Biotechnol* 2014;32(3):223-226.
- 20 Vizcaino JA, Csordas A, del-Toro N, Dienes JA, Griss J, Lavidas I, Mayer G, Perez-Riverol Y, Reisinger F, Ternent T, Xu QW, Wang R, Hermjakob H. 2016 update of the PRIDE database and its related tools. *Nucleic Acids Res* 2015;44(1):D447-D456.
- 21 Deng W, Wang Y, Liu Z, Cheng H, Xue Y. HemI: a toolkit for illustrating heatmaps. *PLoS One* 2014;9(11):e111988.
- 22 Mi H, Muruganujan A, Casagrande JT, Thomas PD. Large-scale gene function analysis with the PANTHER classification system. *Nat Protoc* 2013;8(8):1551-1566.
- 23 Mi H, Muruganujan A, Thomas PD. PANTHER in 2013: modeling the evolution of gene function, and other gene attributes, in the context of phylogenetic trees. *Nucleic Acids Res* 2013;41(Database issue):D377-D386.
- 24 Szklarczyk D, Franceschini A, Wyder S, Forslund K, Heller D, Huerta-Cepas J, Simonovic M, Roth A, Santos A, Tsafou KP, Kuhn M, Bork P, Jensen LJ, von Mering C. STRING v10: protein-protein interaction networks, integrated over the tree of life. *Nucleic Acids Res* 2015;43(Database issue):D447-D452.
- 25 Kanehisa M, Sato Y, Kawashima M, Furumichi M, Tanabe M. KEGG as a reference resource for gene and protein annotation. *Nucleic Acids Res* 2016;44(D1):D457-D462.
- 26 Lachmann A, Xu H, Krishnan J, Berger SI, Mazloom AR, Ma'ayan A. ChEA: transcription factor regulation inferred from integrating genome-wide ChIP-X experiments. *Bioinformatics* 2010;26(19):2438-2444.
- 27 Chen EY, Xu H, Gordonov S, Lim MP, Perkins MH, Ma'ayan A. Expression2Kinases: mRNA profiling linked to multiple upstream regulatory layers. *Bioinformatics* 2012;28(1):105-111.
- 28 Schneider CA, Rasband WS, Eliceiri KW. NIH Image to ImageJ: 25y of image analysis. *Nat Methods* 2012;9(7):671-675.
- 29 Karp NA, Lilley KS. Investigating sample pooling strategies for DIGE experiments to address biological variability. *Proteomics* 2009;9(2):388-397.
- 30 Molloy MP, Brzezinski EE, Hang J, McDowell MT, VanBogelen RA. Overcoming technical variation and biological variation in quantitative proteomics. *Proteomics* 2003;3(10):1912-1919.
- 31 Castañó EM, Roher AE, Esh CL, Kokjohn TA, Beach T. Comparative proteomics of cerebrospinal fluid in neuropathologically-confirmed Alzheimer's disease and non-demented elderly subjects. *Neurol Res* 2006;28(2):155-163.
- 32 Weinkauf M, Hiddemann W, Dreyling M. Sample pooling in 2-D gel electrophoresis: a new approach to reduce nonspecific expression background. *Electrophoresis* 2006;27(22):4555-4558.
- 33 Kwong JQ, Beal MF, Manfredi G. The role of mitochondria in inherited neurodegenerative diseases. *J Neurochem* 2006;97(6):1659-1675.
- 34 Sanges D, Comitato A, Tammaro R, Marigo V. Apoptosis in retinal degeneration involves cross-talk between apoptosis-inducing factor (AIF) and caspase-12 and is blocked by calpain inhibitors. *Proc Natl Acad Sci U S A* 2006;103(46):17366-17371.
- 35 Sedeek M, Nasrallah R, Touyz RM, Hébert RL. NADPH oxidases, reactive oxygen species, and the kidney: friend and foe. *J Am Soc Nephrol* 2013;24(10):1512-1518.
- 36 Komeima K, Rogers BS, Lu L, Campochiaro PA. Antioxidants reduce cone cell death in a model of retinitis pigmentosa. *Proc Natl Acad Sci U S A* 2006;103(30):11300-11305.
- 37 Shen J, Yang X, Dong A, Petters RM, Peng YW, Wong F, Campochiaro PA. Oxidative damage is a potential cause of cone cell death in retinitis pigmentosa. *J Cell Physiol* 2005;203(3):457-464.
- 38 Danial NN, Korsmeyer SJ. Cell death: critical control points. *Cell* 2004;116(2):205-219.
- 39 Krebs HA. The citric acid cycle: a reply to the criticisms of F. L. Breusch and of J. Thomas. *Biochem J* 1940;34(3):460-463.
- 40 Kay J, Weitzman PDJ. Krebs' citric acid cycle: half a century and still turning. *Biochemical Society* 1987.
- 41 Zencak D, Schouwey K, Chen D, Ekstrom P, Tanger E, Bremner R, van Lohuizen M, Arsenijevic Y. Retinal degeneration depends on Bmi1 function and reactivation of cell cycle proteins. *Proc Natl Acad Sci U S A* 2013;110(7):E593-E601.
- 42 Höglinger GU, Breunig JJ, Depboylu C, Rouaux C, Michel PP, Alvarez-Fischer D, Boutillier AL, Degregori J, Oertel WH, Rakic P, Hirsch EC, Hunot S. The pRb/E2F cell-cycle pathway mediates cell death in Parkinson's disease. *Proc Natl Acad Sci U S A* 2007;104(9):3585-3590.